

1 Single cell microscopy reveals that levels of cyclic di-GMP vary among *Bacillus*
2 *subtilis* subpopulations

3

4 **Authors and Affiliations:**

5 Cordelia A. Weiss^a, Jakob A. Hoberg^a, Kuanqing Liu^b, Benjamin P. Tu^b, Wade C.
6 Winkler^a#

7 ^a Department of Cell Biology and Molecular Genetics, University of Maryland, College
8 Park, Maryland, USA

9 ^b Department of Biochemistry, The University of Texas Southwestern Medical Center,
10 Dallas, Texas, USA

11

12 **Running Title: c-di-GMP varies among *Bacillus subtilis* cell types**

13

14 # Address correspondence to Wade C. Winkler, wwinkler@umd.edu

15

16

17

18

19

20

21

22

23

24 **Abstract**

25 The synthesis of signaling molecules is one strategy bacteria employ to sense
26 alterations in their environment and rapidly adjust to those changes. In Gram-negative
27 bacteria, bis-(3'-5')-cyclic dimeric guanosine monophosphate (c-di-GMP) regulates the
28 transition from a unicellular motile state to a multicellular sessile state. However, c-di-
29 GMP signaling has been less intensively studied in Gram-positive organisms. To that
30 end, we constructed a fluorescent *yfp* reporter based on a c-di-GMP-responsive
31 riboswitch, to visualize the relative abundance of c-di-GMP for single cells of the Gram-
32 positive model organism *Bacillus subtilis*. Coupled with cell type-specific fluorescent
33 reporters, this riboswitch reporter revealed that c-di-GMP levels are markedly different
34 among *B. subtilis* cellular subpopulations. For example, cells that have made the
35 decision to become matrix producers maintain higher intracellular c-di-GMP
36 concentrations as compared to motile cells. Similarly, we find that c-di-GMP levels differ
37 between sporulating and competent cell types. These results suggest that biochemical
38 measurements of c-di-GMP abundance are likely to be inaccurate for a bulk ensemble
39 of *B. subtilis* cells, as such measurements will average c-di-GMP levels across the
40 population. Moreover, the significant variation in c-di-GMP levels between cell types
41 hints that c-di-GMP might play an important role during *B. subtilis* biofilm formation. This
42 study therefore emphasizes the importance of using single-cell approaches for
43 analyzing metabolic trends within ensemble bacterial populations.

44

45

46

47 Importance

48 Many bacteria have been shown to differentiate into genetically identical, yet
49 morphologically distinct cell types. Such population heterogeneity is especially prevalent
50 among biofilms, where multicellular communities are primed for unexpected
51 environmental conditions and can efficiently distribute metabolic responsibilities.
52 *Bacillus subtilis* is a model system for studying population heterogeneity; however, a
53 role for c-di-GMP in these processes has not been thoroughly investigated. Herein, we
54 introduce a fluorescent reporter, based on a c-di-GMP-responsive riboswitch, to
55 visualize the relative abundance of c-di-GMP for single *B. subtilis* cells. Our analysis
56 shows that c-di-GMP levels are conspicuously different among *B. subtilis* cellular
57 subtypes, suggesting a role for c-di-GMP during biofilm formation. These data highlight
58 the utility of riboswitches as tools for imaging metabolic changes within individual
59 bacterial cells. Analyses such as these offer new insight into c-di-GMP regulated
60 phenotypes, especially given that other biofilms also consist of multicellular
61 communities.

62

63

64

65

66

67

68

69

70 **Introduction**

71 Bacteria use diverse strategies to sense alterations in their environment and rapidly
72 adjust to those changes. Adaptability to cell stresses can sometimes be manifested as
73 phenotypic variation, where individual cells differentially express subsets of their genes,
74 sometimes occurring within an isogenic population (1–3). For example, in the Gram-
75 positive model microorganism *Bacillus subtilis*, bistability in gene expression can help
76 guide differentiation of distinct cell types (4, 5). Some cells within a bulk *B. subtilis*
77 population express motility genes, as induced by the sigma factor SigD (6).
78 Simultaneously, a smaller subset are activated by the ComK transcription factor to
79 differentiate into competent cells, proficient in DNA uptake and primed for homologous
80 recombination (7). Other cells within the population are triggered by regulatory proteins
81 (e.g., SinR/SinI, SlrR, and DegU) to differentiate into sessile chains that overproduce
82 biofilm matrix components or extracellular proteases (8–11). Yet another subpopulation
83 is irreversibly directed into the developmental program of endospore formation, which
84 culminates in formation of a dormant cell type resistant to many stresses (12, 13). For
85 cells that will be encouraged into endospore formation, nutrient limitation stimulates a
86 phosphorelay that results in phosphorylation of the master regulator Spo0A, which
87 triggers the onset of sporulation. Furthermore, cells that are farther into the sporulation
88 program than others will secrete extracellular killing factors to cannibalize their siblings
89 for nutrients (14). In sum, *B. subtilis* is capable of switching between cell fates through
90 highly coordinated processes that are governed by master regulators, two-component
91 systems, and phosphorylation cascades.

92

93 Signaling molecules also influence *B. subtilis* differentiation pathways. Several types of
94 signaling molecules have been discovered that coordinate gene expression and
95 regulate bacterial behavior. One class of extracellular signaling molecules, called
96 autoinducers, regulate quorum sensing and allow bacterial populations to behave
97 collectively (15). In addition to autoinducers, a variety of nucleotide-based second
98 messengers are specifically produced for intracellular signaling in bacteria (16–18). One
99 particular ribonucleotide signaling molecule, bis-(3'-5')-cyclic dimeric guanosine
100 monophosphate (c-di-GMP), has been shown in many bacteria to regulate the transition
101 from a unicellular motile state to a multicellular sessile community (19, 20). C-di-GMP
102 signaling networks are encoded in almost every phylum in the bacterial domain, making
103 this molecule a near-universal second messenger, although it has still been
104 incompletely examined in several model microbes (21).

105

106 In response to external stimuli, c-di-GMP is synthesized from 2 GTP molecules by
107 GGDEF domain-containing diguanylate cyclases (DGCs) (22–28). The second
108 messenger can then bind intracellular effectors to direct physiological changes. EAL or
109 HD-GYP domain-containing phosphodiesterases (PDEs) hydrolyze cyclic di-GMP into
110 the linear dinucleotide 5'-phosphoguanylyl-(3'-5')-guanosine (pGpG) (29–38), which is
111 then recycled into nucleoside monophosphate pools through the action of
112 oligoribonucleases (39–41)). Through bioinformatic analyses, GGDEF, EAL, and HD-
113 GYP domain containing enzymes have readily been identified in almost all bacterial
114 phyla (35, 42). Conversely, there is greater diversity in the classes of receptors that
115 associate with c-di-GMP. These receptors often have no sequence or structural

116 similarity to one another, making the prediction of c-di-GMP receptors sometimes
117 difficult (43). In addition to the large number of protein receptors, riboswitches also have
118 been shown to bind c-di-GMP to regulate gene expression (44, 45). Riboswitches are
119 located in the untranslated regions of mRNA transcripts and coordinate downstream
120 gene expression in response to highly specific interactions with their cognate ligand
121 (46). The presence of c-di-GMP-responsive riboswitches upstream of a diverse array of
122 genes, such as GGDEF/EAL/HD-GYP proteins, flagella, pili, other motility factors,
123 transcription factors, and membrane transporters suggests many different targets of c-
124 di-GMP regulation in bacteria (47, 48).

125

126 *B. subtilis* encodes three DGCs (DgcK, DgcP, DgcW), one PDE (PdeH), and three
127 putative c-di-GMP receptors (Motl, YdaK, and Ykul) (Supp Fig 1) (49, 50). Motl is a
128 PilZ-domain containing protein that is thought to inhibit flagellar motility by acting as a
129 molecular clutch on the flagellar stator element MotA, to disengage and sequester it
130 from the flagellar rotor FliG (51). Genetic evidence also supports a direct relationship
131 between c-di-GMP and the regulation of motility through Motl and PdeH (49, 50). While
132 deletion of *pdeH* results in a swarming motility defect, it does not result in any obvious
133 changes to biofilm colonies or pellicles. Overexpression of the DGCs did not appear to
134 affect biofilms either, initially suggesting c-di-GMP is not important for control of biofilm
135 formation in this organism. Recently, however, data suggests that the degenerate DGC
136 YdaK is a c-di-GMP receptor that is likely to participate in biofilms. YdaK is encoded
137 within the *ydaJKLMN* operon. While the exact role of the *yda* operon has yet to be
138 determined, the operon may be involved in the synthesis of an unknown

139 exopolysaccharide, which may bolster the stress-resistance of the biofilm under specific
140 physiological conditions (52, 53). Therefore, more remains to be understood regarding
141 the role of c-di-GMP in regulating *B. subtilis* biofilm formation. The third putative
142 receptor, Ykul, is a catalytically inactive PDE that has retained the ability to bind c-di-
143 GMP, but not hydrolyze it (54). Interestingly, its deletion was shown to confer resistance
144 to inhibitory concentrations of zinc (55). It is possible that deletion of *yku* somehow
145 restricts access to zinc, although a mechanistic model for this phenotype has yet to be
146 identified. Furthermore, its involvement in regulation of lifestyle switching in *B. subtilis*
147 has not yet been ascertained.

148

149 The genetic malleability and wealth of knowledge regarding *B. subtilis* development
150 make it an excellent experimental model in which to interrogate the contribution of c-di-
151 GMP regulation to cell differentiation in Firmicutes. Elevated c-di-GMP levels have been
152 shown to inhibit motility in this organism (49, 50); however, it is currently unknown if
153 sporulation and competence are also regulated by this signaling molecule. Developing
154 evidence suggests that c-di-GMP may also affect the composition of extracellular
155 polysaccharides during biofilm formation in this organism (52, 53). Yet the methods
156 used to examine whether c-di-GMP affects biofilm formation have thus far incompletely
157 considered that *B. subtilis* biofilms are heterogeneously composed of several sub-
158 populations (4, 5, 56). In this study, we made use of a fluorescent c-di-GMP-responsive
159 riboswitch reporter and quantified its expression *in vivo* for single cells of *B. subtilis*.
160 When combined with fluorescent transcriptional reporters that demarcate the primary
161 classes of cell types, the c-di-GMP riboswitch reporter displayed markedly different

162 levels of fluorescence within the multicellular community. The combination of these data
163 revealed that within a single population, some cell fates correlate with high levels of c-
164 di-GMP while other fates exhibit low c-di-GMP. Therefore, these data demonstrate that
165 for some bacteria c-di-GMP levels are adjusted heterogenously across bulk populations.
166 Finally, these data highlight the utility of riboswitches as tools for imaging metabolic
167 changes within individual bacterial cells.

168

169 **Results**

170 Analysis of a c-di-GMP-responsive riboswitch upstream of *B. licheniformis* lichenysin 171 synthesis genes

172 In this study, we sought to identify a riboswitch that could be used to construct a genetic
173 reporter of c-di-GMP. A bioinformatics-based search for c-di-GMP-responsive
174 riboswitches in Bacillales revealed a particularly interesting candidate in the
175 untranslated leader region of the *Bacillus licheniformis* *lch* gene cluster. This nearly 27
176 kb operon (*lchA*) encodes the subunits of the nonribosomal peptide synthetase that
177 makes lichenysin. Lichenysin is an antimicrobial cyclic lipopeptide that is virtually
178 identical to surfactin, an important specialized metabolite produced by *B. subtilis* (57–
179 59). The location of this riboswitch is particularly interesting given that riboswitches have
180 not been previously analyzed as being important for genetic regulation of secondary
181 metabolites. We chose to further examine this class I riboswitch to determine whether it
182 is a good candidate for development of a genetic reporter of c-di-GMP abundance.

183

184 The interaction between a riboswitch and its cognate ligand induces a conformational
185 change in the transcript that modulates downstream gene expression (60). Many
186 riboswitches couple detection of their target signal to transcription attenuation. In the
187 unbound state, these riboswitches will oftentimes adopt a conformation in which an
188 “anti-terminator” helix is created from the left half of the terminator and an upstream
189 sequence. Then, when bound to its cognate ligand, the riboswitch will adopt an
190 alternate conformation that allows for formation of an intrinsic terminator (61), causing
191 disassociation of the transcription elongation complex (Fig 1A). Manual inspection of the
192 *IchAA* putative riboswitch revealed that its sequence included a candidate terminator
193 site. Therefore, to determine if c-di-GMP modulates downstream gene expression of the
194 putative *B. licheniformis* riboswitch, we performed a transcription termination assay *in*
195 *vitro* (Fig 1B). A DNA template of the *IchAA* untranslated element that included 50
196 nucleotides beyond the putative terminator (“run-off”) was generated by PCR and mixed
197 with RNA polymerase holoenzyme in the presence of varying amounts of c-di-GMP.
198 Under the conditions that we used, a concentration of 10 µM c-di-GMP began to
199 promote transcription termination at the terminus of the riboswitch, and ligand-
200 responsive termination continued to increase up to the maximum concentration tested,
201 1 mM c-di-GMP.

202

203 To directly measure binding of c-di-GMP to the *IchAA* riboswitch, we identified the *IchAA*
204 aptamer domain via manual inspection and fused it to the Spinach2 aptamer. Spinach
205 and Spinach2 RNAs fluoresce upon binding 3,5-difluoro-4-hydroxybenzylidene
206 imidazolinone (DFHBI) (62, 63). Spinach variants can be carefully fused to riboswitch

207 aptamer domains such that the Spinach domain fluoresces only in response to binding
208 of the riboswitch ligand (64–66). Therefore, we isolated the *lchAA* aptamer and fused it
209 to the P2 stem loop of Spinach2 (Supp Fig 2). We hypothesized this would create an
210 allosteric version of Spinach2, thereby creating an RNA with two distinct binding sites,
211 for which binding of the *lchAA* aptamer to its cognate ligand will then trigger binding of
212 DFHBI to Spinach2 (Fig 1C). We then measured Spinach2 fluorescence in the presence
213 of saturating concentrations of DFHBI and with increasing concentrations of c-di-GMP.
214 This revealed that fluorescence of the *lchAA* aptamer-Spinach2 RNA was dependent on
215 an appropriate amount of c-di-GMP, confirming that the *lchAA* aptamer acts as a sensor
216 of c-di-GMP. In contrast, we did not detect Spinach2 fluorescence in the presence of
217 100 μ M c-di-AMP. The *lchAA* aptamer, as part of a Spinach2 biosensor construct,
218 bound c-di-GMP with an apparent K_d of 17 nM. While this apparent K_d is lower than the
219 concentration of c-di-GMP required to promote transcription termination *in vitro* on
220 purified DNA templates, it has been observed that many riboswitches are not driven by
221 equilibrium ligand interactions. Instead, many riboswitches are driven by coordination of
222 the kinetics of ligand association and RNA polymerization speed (67). In these
223 instances, a higher concentration of c-di-GMP is required to promote a conformational
224 change of the expression platform *in vitro*. Fluorescence of the *lchAA*-Spinach2 aptamer
225 was also observed in the presence of pGpG, the linear dinucleotide and c-di-GMP
226 degradation product; however, the apparent K_d for this molecule was two orders of
227 magnitude higher than that for c-di-GMP (Fig 1D). This roughly agrees with previous
228 results in which pGpG binds a c-di-GMP riboswitch with much poorer affinity (68). We

229 conclude from these aggregate data that c-di-GMP specifically interacts with the *IchAA*
230 riboswitch to promote transcription attenuation of the *IchAA* operon.

231

232 A c-di-GMP riboswitch-yfp reporter is heterogeneously expressed in *B. subtilis*

233 We next wanted to assess c-di-GMP levels in single cells of *B. subtilis* *in vivo*. Since
234 intracellular expression of Spinach has not been examined for this organism, we first
235 ectopically integrated a constitutively expressed Spinach2 sequence into the *B. subtilis*
236 PY79 genome at a nonessential locus. When cells reached late-log ($OD_{600}=1.0$), they
237 were incubated with saturating DFHBI for one hour and examined by fluorescence
238 microscopy. These cells exhibited a roughly two-fold increase in fluorescence as
239 compared to untreated cells. However, many cells remained fully inactivated for
240 fluorescence in the presence of DFHBI, indicating broad heterogeneity in fluorescence
241 by a constitutive Spinach2 reporter (Supp Fig 3). Incubation with DFHBI for one hour
242 seemingly had no effect on bacterial growth, either for cells in culture or upon
243 examination by microscopy.

244

245 As the Spinach2-based reporter was unacceptably non-uniform in *B. subtilis*, we
246 constructed a reporter based on expression of YFP. We ectopically integrated a
247 constitutively expressed *yfp* sequence into the *B. subtilis* genome and analyzed cells at
248 late-log ($OD_{600}=1.0$) by fluorescence microscopy. Unlike the strain that constitutively
249 expressed Spinach2, the constitutive *yfp* strain exhibited more uniform fluorescence.
250 This population exhibited a unimodal distribution of fluorescence per cell (Fig 2A, B).
251 We then constructed a corresponding reporter based on the c-di-GMP riboswitch. The

252 entire leader sequence of *B. licheniformis* *lchAA* was inserted between the constitutively
253 active promoter sequence and *yfp*. Unlike the constitutive *yfp* reporter, a strain
254 containing the riboswitch-*yfp* reporter exhibited two prominently distinct levels of
255 fluorescence within the population. Nearly 70% of the cells were moderately fluorescent
256 as compared to the constitutive *yfp* strain, while the remaining cells exhibited
257 significantly diminished fluorescence (Fig 2A, B). Therefore, unlike the unimodal
258 distribution of fluorescence exhibited by the constitutive *yfp* reporter, the riboswitch-*yfp*
259 reporter strain appeared to show a bimodal distribution of fluorescence. To determine
260 whether this distribution was due to riboswitch regulation of YFP, we mutated the
261 riboswitch element. Specifically, we deleted 65 nucleotides from the 5' end of the *lchAA*
262 leader, which includes part of the c-di-GMP-binding aptamer, and re-examined cellular
263 fluorescence. This population of cells uniformly expressed YFP at levels similar to the
264 constitutive *yfp* reporter construct (Fig 2A, C). Long considered a *B. subtilis* "legacy"
265 laboratory strain, PY79 has been widely used in a plethora of genetic analyses that
266 have provided profound insight into the molecular pathways that govern cellular
267 differentiation. Indeed, the regulation of cell-specific gene expression in *B. subtilis* was
268 determined in this genetic background (69–74). Historically, however, undomesticated
269 strains such as 3610 have often been used to study biofilm formation (10, 75–77). We
270 therefore also assessed our riboswitch-*yfp* reporter in the undomesticated 3610
271 background. We observed an identical distribution of fluorescence to the PY79
272 background, suggesting that c-di-GMP dynamics behave similarly in both strains (Supp
273 Fig 4). Therefore, we chose to continue our studies with PY79 for interrogating gene
274 expression differences between different cellular sub-types. Taken together, these

275 findings suggest that the c-di-GMP riboswitch-*yfp* reporter is bimodally expressed in a
276 population of *B. subtilis*.

277

278 The riboswitch reduces downstream gene expression in response to elevated c-di-GMP

279 Of the two phosphodiesterases encoded in the *B. subtilis* genome, previous work has
280 shown only PdeH to be active (49, 50). With this in mind, we wanted to confirm that the
281 bimodal distribution of fluorescence observed in single cells of *B. subtilis* was solely due
282 to differences in intracellular c-di-GMP levels. To do this, we integrated the constitutive
283 *yfp* and riboswitch-*yfp* reporter fusions into a Δ*pdeH* knockout strain. We predicted that
284 loss of PdeH should inhibit hydrolysis of c-di-GMP and consequently elevate
285 intracellular levels, which should promote premature transcription termination in the
286 riboswitch-*yfp* reporter fusion, thereby reducing YFP signal. Indeed, the riboswitch-*yfp*
287 reporter resulted in significantly decreased *yfp* expression in the Δ*pdeH* background,
288 suggesting intracellular cyclic di-GMP was elevated in all cells at late-log phase
289 (OD₆₀₀=1.0) (Fig 3B, D). Conversely, constitutive *yfp* expression was unaffected by the
290 Δ*pdeH* mutation, confirming the specificity of the riboswitch-*yfp* reporter for c-di-GMP
291 (Fig 3A, C).

292

293 To independently assess the contribution of PdeH to c-di-GMP in cells, we employed
294 liquid chromatography-tandem mass spectrometry (LC-MS/MS) to detect c-di-GMP
295 levels in both PY79 wild-type and Δ*pdeH*, grown to late-log phase (OD₆₀₀=1.0). A
296 roughly 3-fold increase in c-di-GMP was observed by LC-MS/MS for the bulk population
297 of Δ*pdeH* cells (Supp Fig 5). We also attempted to quantify intracellular pGpG levels,

298 but levels of pGpG were below the limit of detection for both wild-type and $\Delta pdeH$ cells
299 (data not shown). A previous study quantified intracellular pGpG by LC-MS/MS in a *B.*
300 *subtilis* mutant devoid of NrnA and NrnB, which are the two exoribonucleases thought to
301 degrade pGpG in Firmicutes and other organisms that do not encode Oligoribonuclease
302 (Orn) (41). Similar to our current study, pGpG was undetectable in wild-type cells and
303 could only be detected in the $\Delta nrrA \Delta nrrB$ double mutant. Therefore, we conclude that
304 pGpG does not accrue to levels high enough to interfere with the c-di-GMP riboswitch-
305 *yfp* reporter.

306

307 Expression of the riboswitch reporter correlates with specific cell types

308 We next sought to correlate c-di-GMP levels with subpopulations of *B. subtilis*. We
309 replaced *yfp* with another gene encoding for a red fluorescent protein, mCherry, and
310 introduced the riboswitch reporter in strains that already harbored transcriptional *gfp* or
311 *yfp* reporters that demarcate the most common *B. subtilis* cell types including: motile,
312 matrix-producing, or competent. When analyzed by fluorescence microscopy at late-log
313 phase ($OD_{600}=1.0$), a majority of cells exhibited high expression of a $P_{hag}-gfp$ reporter
314 (denoting motility) and high expression of the riboswitch-*mCherry* reporter (signifying
315 low c-di-GMP). Of the cells that were transcriptionally active for motility gene
316 expression, 89.8% also exhibited fluorescence from the riboswitch reporter. This
317 suggests that c-di-GMP abundance is uniformly low in motile cells (Fig 4A, D), and that
318 a positive correlation exists between the genetic reporters. Low c-di-GMP levels were
319 also observed in competent cells. While roughly 20% of cells in the population were
320 competent, as indicated by a $P_{comG}-yfp$ reporter, 79.7% of these cells exhibited high

321 fluorescence from the c-di-GMP riboswitch-*mCherry* reporter (Fig 4C, F). However,
322 when we analyzed the riboswitch-*mCherry* reporter in the context of matrix-producing
323 cells, as identified by a P_{tapA} -*yfp* reporter, we observed an anti-correlation between both
324 reporters. Cells activated for producing extracellular matrix (as denoted by *tapA* gene
325 expression) were observed mainly as long chains. Of these activated cells, 81.0%
326 exhibited diminished fluorescence from the riboswitch-*mCherry* reporter (Fig 4B, E).
327 This suggests that c-di-GMP levels are high in matrix-producing cells. Conversely, cells
328 that showed high fluorescence for the riboswitch-*mCherry* reporter were almost never
329 activated for *tapA* expression. We did, however, observe a small population of cells that
330 had c-di-GMP levels sufficiently high enough to shut off the riboswitch reporter, but that
331 had not activated the transcriptional reporter for biofilm formation (P_{tapA} -*yfp*). We
332 speculate that these cells had not been activated yet for extracellular matrix production,
333 which might suggest that c-di-GMP levels change prior to activation of matrix
334 production. Finally, we introduced the riboswitch-*yfp* reporter in a strain that also
335 harbored a P_{const} -*mCherry* reporter and assessed c-di-GMP levels in cells that were
336 activated for sporulation. Cells that progressed through spore development maintained
337 expression of *mCherry*, but were uniformly low in riboswitch-*yfp* expression, suggesting
338 that c-di-GMP levels are high during endospore formation (Fig 5).

339

340 An increase in c-di-GMP does not appear to change cell type identity
341 To see if the manipulation of intracellular c-di-GMP levels could influence the proportion
342 of cells that became matrix producers (as well as motile or competent). We used the
343 “high c-di-GMP” strain, $\Delta pdeH$, and integrated both transcriptional reporters for c-di-

344 GMP levels and cell type in this background. When cells were analyzed by fluorescence
345 microscopy, we observed uniformly low mCherry levels of fluorescence, thereby
346 confirming the elevated levels of c-di-GMP in the $\Delta pdeH$ strain (Fig 6). Additionally, we
347 observed no obvious consequence on cell fate at the transcriptional level. In many
348 instances, however, c-di-GMP regulates phenotypic outputs at the post-translational
349 level (78–80). This is exemplified in *B. subtilis* motile cells, where the binding of MotI to
350 c-di-GMP directs MotI to directly disengage MotA from the rotor of the flagellar
351 apparatus (51). It is possible that c-di-GMP post-translationally regulates YdaK as well,
352 and this interaction activates production of the unknown EPS. So, while the proportion
353 of cells in each sub-type was consistent between the wild-type and $\Delta pdeH$ mutant, and
354 the level of activation for motility and matrix gene expression as measured by the
355 reporters was the same (Fig 6A-B, D-E), it remains possible that c-di-GMP could be a
356 regulator of *B. subtilis*' differentiation at the post-translational level. Interestingly, mild
357 repression of the competence transcriptional reporter was observed in the $\Delta pdeH$ strain
358 as compared to wild-type (Fig 6C, F).

359

360 *pdeH* expression is regulated transcriptionally

361 In addition to the catalytic EAL domain that provides phosphodiesterase activity, some
362 PDEs also contain sensory domains (e.g. PAS) that allow for post-translational
363 regulation of phosphodiesterase activity through activation by an extracellular signal. No
364 such domain has been identified in *B. subtilis* *PdeH*. However, *pdeH* transcription was
365 previously suggested to be repressed by Spo0A (49, 81) indicating that *pdeH* might be
366 regulated transcriptionally. We therefore sought to ascertain if heterogeneous

expression of the riboswitch reporter was due to heterogeneous expression of *pdeH* in each cellular sub-type. We created a transcriptional fusion of the *pdeH* promoter to a reporter gene encoding Superfolder GFP ('P_{*pdeH*}-sf gfp') and ectopically integrated it into wild-type and Δ *spo0A* background strains. Mean fluorescence for the Δ *spo0A* background (0.162, 95% CI 0.158-0.167) increased by roughly 2-fold as compared to wild-type (0.086, 95% CA 0.082-0.090) (Fig 7A). This agrees with prior data showing Spo0A inhibition of *pdeH* expression (49). Furthermore, quantification of the P_{*pdeH*}-sf gfp reporter revealed a single peak, implying a normal distribution of *pdeH* expression across the population. While a Δ *sigD* mutation had little effect on mean fluorescence (0.075, 95% CI 0.071-0.080) (Fig 7C), a Δ *sinR* mutation (0.050, 95% CI 0.046-0.054) led to a roughly 2-fold decrease in mean fluorescence (Fig 7B). From this, we speculate that removal of SinR might lead to physiological changes that enhance activation of Spo0A, thereby maximizing the Spo0A-mediated inhibition of *pdeH* transcription. Alternatively, it is possible that SinR might activate expression of *pdeH*, directly or indirectly, through an unknown mechanism. We also quantified fluorescence from the riboswitch reporter in these genetic backgrounds to correlate c-di-GMP levels with activity from *pdeH*. Our data (Fig 7A-C) predicts that de-repression of *pdeH* due to Δ *spo0A* should lead to lower intracellular c-di-GMP, exhibited by uniformly high fluorescence from the riboswitch reporter. Conversely, repression of *pdeH* due to Δ *sinR* should result in higher intracellular c-di-GMP and result in uniformly lower fluorescence from the riboswitch reporter. As predicted, our riboswitch reporter followed the hypothesized trends. A Δ *spo0A* mutation led to loss of a bimodal distribution of fluorescence, and the population exhibited similar fluorescence to the "low c-di-GMP"

390 population of wild-type (Fig 7D). Mean fluorescence in a $\Delta sinR$ mutant was uniformly
391 low (0.023, 95% CI 0.022-0.023), indicating high intracellular c-di-GMP (Fig 7E).
392 Unexpectedly, however, we observed uniformly low fluorescence from the riboswitch
393 reporter in a $\Delta sigD$ background (0.029, 95% CI 0.028-0.030). This suggests $\Delta sigD$ cells
394 have an increase in intracellular c-di-GMP that cannot be explained by *pdeH* activity
395 alone (Fig 7C, F).

396

397 **Discussion**

398 In order to study c-di-GMP abundance for single cells of *B. subtilis*, we employed a
399 constitutively expressed c-di-GMP riboswitch fused to *yfp* as our biosensor. This
400 riboswitch reporter revealed apparent differences in intracellular c-di-GMP levels among
401 *B. subtilis* sub-populations. From these results, we suggest that c-di-GMP riboswitch-*yfp*
402 reporters could be used in other bacteria—Bacillales in particular—for single cell
403 analyses of c-di-GMP abundance. These riboswitch-reporters may prove to be useful
404 tools in elucidating the increasingly diverse c-di-GMP regulatory mechanisms used by
405 Gram-positive bacteria. Studies on *Bacillus cereus* group organisms, *Clostridioides*
406 *difficile*, and *Streptomyces coelicolor* have suggested a link between c-di-GMP
407 metabolism and spore formation, which is a developmental program almost exclusive to
408 the three genera (20). Interestingly, there is an ortholog of *B. subtilis* Ykul in the *B.*
409 *cereus* bacterial group, which is named *CdgJ*. Overexpression of *B. thuringiensis* *cdgJ*
410 resulted in increased biofilm formation and earlier entry into sporulation (82).
411 Conversely, no sporulation was observed in a *B. thuringiensis* *cdgJ* mutant. Given the
412 high similarity in protein sequences between Ykul and *CdgJ*, it is therefore possible that

413 Ykul might also exhibit a similar role in *B. subtilis*, although it has yet to be explored.

414 Sporulation is also affected by c-di-GMP in *S. coelicolor*. Overexpression of DGCS *cdgA*

415 or *cdgB*, or deletion of PDEs *rmdA* or *rmdB* led to an increase in intracellular c-di-GMP

416 and inhibition of sporulation (83–85). Studies on *S. coelicolor* have also revealed the

417 only c-di-GMP-sensing, transcriptional regulator to date among Gram-positive

418 organisms (*BldD*). Deletion of *bldD* accelerates sporulation (86) which is inhibited

419 through overexpression of *cdgA* and *cdgB*, which are also direct targets of *BldD*. C-di-

420 GMP-bound *BldD* also represses expression of antibiotic synthesis genes and

421 sporulation genes during vegetative growth (83, 84). Together, these studies generally

422 suggest a broadening role for c-di-GMP signaling in Gram-positive bacteria. Our study

423 herein extends this even further by showing that a c-di-GMP riboswitch is likely to

424 control expression of a *B. licheniformis* lichenysin biosynthesis gene cluster. This

425 observation suggests that in some bacteria antibiotic synthesis is under the purview of

426 c-di-GMP signaling. By extension, these data suggest that surfactin biosynthesis could

427 also be subjected to c-di-GMP regulation in other *Bacillus* species. Interestingly, a

428 peptide essential for competence (*ComS*) is encoded within the surfactin operon *srfAA-*

429 *AD* in *B. subtilis* (87). *srfAA-AD* is also regulated by the transcription factor *ComA*,

430 which is ultimately activated by the quorum sensing molecule *ComX* (88–90). This

431 regulatory arrangement allows *B. subtilis* to integrate a single signaling pathway into

432 multiple adaptive processes. Prior studies have shown that surfactin-producing cells

433 coexist with, but are phenotypically distinct from, cells that produce the extracellular

434 matrix components (91). Therefore, our observation that c-di-GMP is low in competent

435 cells implies that c-di-GMP should also be low for surfactin-producing cells. Indeed, the

436 presence of the c-di-GMP riboswitch upstream of *B. licheniformis IchAA* operon
437 indicates that lichenysin is only produced when c-di-GMP levels are low. ComA has
438 been shown to also recognize the *B. licheniformis IchAA* promoter, further supporting a
439 relationship between lichenysin and competence gene expression (92, 93). While a c-di-
440 GMP-responsive riboswitch does not seem to be located in the leader of *B. subtilis*
441 *srfAA*, it is possible that c-di-GMP could regulate this gene cluster by an as yet
442 undiscovered mechanism. In summary, c-di-GMP influences a variety of cellular
443 functions in Gram-positive bacteria, including sporulation and secondary metabolite
444 production and these discoveries may also foreshadow roles for c-di-GMP signaling
445 during competence development in *B. subtilis*.

446
447 Other types of highly selective fluorescent c-di-GMP biosensors have also been
448 developed in recent years. For example, a protein biosensor for c-di-GMP was
449 previously developed from the *Salmonella typhimurium* c-di-GMP binding protein YcgR
450 (94, 95), which coupled binding of c-di-GMP to FRET (Förster Resonance Energy
451 Transfer). This genetically encoded biosensor protein was previously used for FRET-
452 based microscopy of Gram-negative organisms such as *Caulobacter crescentus* and
453 *Pseudomonas aeruginosa* (94, 96). However, FRET-based biosensors exhibit lowered
454 fluorescence intensities compared to individual fluorescent proteins, which can result in
455 an overall narrowing of their dynamic range. Furthermore, many c-di-GMP protein
456 receptors remain to be discovered in Gram-positive organisms for use in FRET
457 microscopy. Riboswitch aptamers have also been used in prior studies as allosteric
458 regulators of the conditionally fluorescent Spinach RNA for measuring c-di-GMP

459 dynamics (64, 97). Yet, while they exhibit ideal performance characteristics *in vitro*, they
460 require further optimization for routine usage in bacterial cells. For example, Spinach-
461 based biosensors exhibit lower fluorescence than common fluorescent proteins. Also,
462 significant amounts of DFHBI have to be added to cells for sufficient quantities of the
463 chromophore to pass through the cell membrane. Some researchers have
464 circumvented this limitation by tagging targeted RNAs with up to 64 spinach aptamers in
465 tandem, thereby increasing the brightness of tagged RNA molecules (98); yet, this
466 approach is not ideal for biosensor purposes. In our experiments, we found that the
467 constitutive YFP control in *B. subtilis* displayed more uniform fluorescence in a
468 population of *B. subtilis* than the constitutive Spinach aptamer (Supp Fig 3). Based on
469 all of these considerations, we chose to pursue development of a riboswitch-yfp reporter
470 fusion that could provide useful information on *B. subtilis* c-di-GMP abundance. The
471 fluorescent proteins used in this study have also been used in multiple studies regarding
472 *B. subtilis* cell differentiation (99, 100). They have been shown to exhibit a shortened
473 half-life and therefore can be expected to report relative differences in gene expression;
474 however, it remains to be determined whether these reporters are sufficient to measure
475 rapid c-di-GMP dynamics.

476
477 Given the importance of *B. subtilis* as a model system for the study of bacterial
478 development, it is essential that its c-di-GMP regulatory mechanisms be further
479 elucidated. One of the most common assays to measure the impact of mutations, such
480 as those affecting c-di-GMP homeostasis, on biofilm formation is to visually assess the
481 complexity of colony topology. While this can be qualitatively useful, it may not be

482 representative of changes that occur at the cellular level. We take this to be due to the
483 inherently heterogeneous composition of cell types within biofilm communities. Instead,
484 the recent development of cell type-specific fluorescent reporters allows investigators to
485 examine features of *B. subtilis* subpopulations and their relationship to c-di-GMP
486 effector proteins, DGCS, and PDEs. (51–53).

487

488 Herein, we couple cell type-specific transcriptional reporters with a c-di-GMP riboswitch-
489 *yfp* reporter to ascertain whether c-di-GMP varies between *B. subtilis* subpopulations.
490 Indeed, our single cell microscopy shows definitively that intracellular c-di-GMP differs
491 among *B. subtilis* cell types within a single population. Cells that have made the
492 decision to become matrix producers maintain higher intracellular c-di-GMP as
493 compared to motile cells. This study also shows that the transition into endospore
494 formation correlates with high c-di-GMP levels, while competent cells correlate with
495 lower c-di-GMP levels. This trend has not been previously examined in other studies.
496 However, while our data demonstrate that c-di-GMP levels vary significantly between
497 different cell types, it is unclear whether these changes in c-di-GMP abundance occur
498 as a result of cellular decision-making or whether they participate in initiating the choice
499 of cell fate. Instead, we provide evidence that a general increase in c-di-GMP
500 abundance is not likely to change the proportion of each cell type at the transcriptional
501 level. While our data suggests that c-di-GMP metabolic enzymes act downstream of the
502 master regulators that drive genetic regulation of cellular differentiation such as Spo0A
503 and SinR (Fig 7A, B), the molecular details of how c-di-GMP levels affect cellular
504 differentiation require further exploration. Indeed, the general importance of c-di-GMP

505 has yet to be fully ascertained for this organism. It is possible that the primary purpose
506 of c-di-GMP signaling in this organism is to influence the motility apparatus.
507 Alternatively, it is possible that effector targets for c-di-GMP-binding proteins have yet to
508 be identified, as might be suggested by the recently discovered link to the *yda*
509 exopolysaccharide pathway (52, 53). Overall, abundance of c-di-GMP in a bulk
510 ensemble of *B. subtilis* is likely averaged across the population and propose that single
511 cell analysis of c-di-GMP levels offers unique insight into how the abundance of this
512 signaling molecule varies among cellular subpopulations. Analyses such as these are
513 likely to offer new insight into c-di-GMP regulated phenotypes, especially given that
514 other biofilms also consist of multicellular communities.

515

516 **Materials and Methods**

517 *Transcription termination assay*

518 PCR amplification was performed on the *B. licheniformis* *lchAA* leader sequence using
519 primers that place it downstream of a constitutive promoter P_{const} and that ended 216
520 nts downstream of the transcription start site (Supp Fig 2). Transcription reactions were
521 performed on the PCR-generated DNA template, resulting in a terminated (T) transcript
522 of approximately 174-nt, or a 217-nt run-off (RO) transcript. These reactions comprised
523 5 μM template, 250 uM NTPs, 1X *E. coli* RNA Polymerase Reaction Buffer (NEB- 40
524 mM Tris-HCl pH 7.5, 150 mM KCl, 10 mM MgCl₂, 1 mM DTT, 0.01% Triton X-100), 20
525 μCi α-³²P-UTP, and 0.5 units of *E. coli* RNA Polymerase, Holoenzyme (NEB). C-di-GMP
526 was added to the run-off transcription reactions to a final concentration of 10 μM, 100
527 μM, and 1 mM. A 125-nt size marker was also transcribed. All reactions were incubated

528 at 37°C for 2 hours. Reactions were resolved by 6% urea-denaturing polyacrylamide gel
529 electrophoresis (PAGE).

530

531 *Spinach Activation Assay*

532 PCR was performed to amplify two aptamers: a tRNA^{Lys}-IchAA-Spinach2 template, and
533 a tRNA^{Lys}-Spinach 2 control template (Supp Fig2). A forward annealing primer was
534 used to introduce the T7 promoter sequence, resulting in a 230-bp and 168-bp DNA
535 template, respectively. Transcription reactions were performed, purified, and quantified
536 as previously described (101). The *in vitro* Spinach2 fluorescence activation assay was
537 modified from methods described previously (64). Briefly, the two RNA aptamers were
538 each diluted to 2 μM and added to an equal volume of 2X renaturation buffer (80 mM
539 HEPES pH 7.5, 250 mM KCl, 6 mM MgCl₂), heated to 70°C for 3 minutes, and cooled at
540 room temperature for 5 minutes. To test binding affinity of c-di-GMP for the *IchAA*
541 aptamer, binding reactions were prepared for each RNA aptamer (40 mM HEPES pH
542 7.5, 125 mM KCl, 3 mM MgCl₂, 100 nM RNA, 10 μM DFHBI) and incubated in the dark
543 at room temperature for 30 minutes. Stocks of c-di-GMP or pGpG were prepared and
544 added to the binding reaction every 30 minutes to achieve the final concentrations that
545 are graphed. Ligands were added until saturation of fluorescence was reached. A
546 Quantus™ Fluorometer (Promega) was used to excite the reaction at 495 nm every 30
547 minutes after incubation with increasing amounts of c-di-GMP and pGpG. Binding to c-
548 di-AMP was also assessed. The experiment was replicated twice, and the background
549 fluorescence of DFHBI alone was subtracted from all data points.

550

551 *Culture conditions and construction of B. subtilis strains*

552 All *B. subtilis* strains in this study are derived from PY79 (unless otherwise noted) and

553 are listed in Table S1. Assessment of *B. subtilis* 3610 was performed with the use of

554 DS7187, a competent 3610 Δ *comI* mutant (provided by D. Kearns, Indiana University)

555 (102). A table of primers and plasmids used is available upon request. Strains were

556 grown at 37°C on Lysogeny Broth (LB) plates supplemented with 1.5% Bacto Agar and

557 when appropriate, with final concentrations of the following antibiotics: 5 µg/mL

558 chloramphenicol, and 1 µg/mL erythromycin added alongside 25 µg/mL lincomycin

559 (mls). Integration at the *amyE* locus was performed with plasmids derived from pJG019

560 (GenBank: KX499653.1), or pVMZ006, both derivatives of pDG1662 (BGSC). To

561 construct pRSL_F4, the *lchAA* leader sequence was synthesized (GenScript) and

562 subcloned into the HindIII restriction site of pJG019. For construction of the P_{pdeH} -sf *gfp*

563 reporter, the constitutive promoter of pVMZ006 was replaced with the $pdeH$ promoter

564 sequence that has been described previously (49). The sequence of sf- *gfp* was

565 amplified from pJ204:102624 (DNA2.0, Inc.) and was used to replace the *yfp* sequence

566 of pVMZ006 via Gibson assembly (103). The fluorescent transcriptional cell-type

567 reporters P_{hag} -*gfp*, P_{tapA} -*yfp*, and P_{comG} -*yfp* that were used in this study have been

568 described previously (4, 5, 104, 105). To construct the plasmids harboring these

569 reporters, promoter sequences of *tapA* and *comG* were amplified from *B. subtilis* and

570 used to replace the constitutive promoter upstream of *yfp* in pVMZ006 by Gibson

571 assembly (103). The *amyE*: P_{hag} -*gfp* fusion from DS4432 (provided by D. Kearns,

572 Indiana University) was introduced into the PY79 chromosome through double

573 homologous recombination of competent cells. Plasmids derived from pDG1664

574 (BGSC) were used for integration at the *thrC* locus. To make markerless deletions of
575 $\Delta pdeH$, $\Delta spo0A$, $\Delta sinR$, and $\Delta sigD$, strains harboring an erythromycin-resistance
576 cassette inserted in loci BSU31740 (*pdeH*), BSU24220 (*spo0A*), BSU24610 (*sinR*), and
577 BSU16470 (*sigD*) were obtained from the BKE collection (BGSC). Markerless deletions
578 were created through transformation with pDR244 (BGSC), as previously described
579 (106). Removal of the erythromycin-resistance cassette was verified by Sanger
580 sequencing. Transformation of PY79 was performed using a previously described
581 protocol (107).

582

583 *Fluorescence microscopy & quantification*

584 Single colonies were used to inoculate liquid MSgg medium (75) and grown at 37°C
585 shaking overnight. The following morning, cultures of each strain were inoculated 1:50
586 in fresh medium and grown at 37°C shaking until reaching an optical density at 600 nm
587 (OD₆₀₀) of 1.0. Aliquots of these cultures were placed on 1.5% low-melting agarose
588 MSgg pads and allowed to dry for 10 minutes. Agarose pads were inverted onto a glass
589 bottom dish (Willco Wells). Cells were imaged at room temperature using a Zeiss Axio-
590 Observer Z1 inverted fluorescence microscope, equipped with a Rolera EM-C₂ electron-
591 multiplying charge-coupled (EMCC) camera, enclosed within a temperature-controlled
592 environmental chamber. Fluorescence intensity per cell was quantified using Oufti
593 analysis software (108). Images were analyzed and adjusted with FIJI software (109).

594

595 **Acknowledgements**

596 Research for this project has been supported by NSF MCB1051440 and NIH AI110432.

597 C.A.W. was supported by NIH T32 GM080201.

598 **References**

- 599 1. Dubnau D, Losick R. 2006. Bistability in bacteria. *Molecular Microbiology* 61:564–572.
- 600 2. Smits WK, Kuipers OP, Veening J-W. 2006. Phenotypic variation in bacteria: the role of
601 feedback regulation. *Nature Reviews Microbiology* 4:259–271.
- 602 3. Veening J-W, Smits WK, Kuipers OP. 2008. Bistability, Epigenetics, and Bet-Hedging in
603 Bacteria. *Annu Rev Microbiol* 62:193–210.
- 604 4. Lopez D, Vlamakis H, Kolter R. 2009. Generation of multiple cell types in *Bacillus subtilis*.
605 *FEMS Microbiology Reviews* 33:152–163.
- 606 5. Vlamakis H, Aguilar C, Losick R, Kolter R. 2008. Control of cell fate by the formation of an
607 architecturally complex bacterial community. *Genes & Development* 22:945–953.
- 608 6. Kearns DB, Losick R. 2005. Cell population heterogeneity during growth of *Bacillus subtilis*.
609 *Genes Dev* 19:3083–3094.
- 610 7. Leisner M, Stingl K, Frey E, Maier B. 2008. Stochastic switching to competence. *Current
611 Opinion in Microbiology* 11:553–559.
- 612 8. Chai Y, Chu F, Kolter R, Losick R. 2008. Bistability and biofilm formation in *Bacillus subtilis*.
613 *Molecular Microbiology* 67:254–263.
- 614 9. Davidson FA, Seon-Yi C, Stanley-Wall NR. 2012. Selective Heterogeneity in Exoprotease
615 Production by *Bacillus subtilis*. *PLOS ONE* 7:e38574.

- 616 10. Kearns DB, Chu F, Branda SS, Kolter R, Losick R. 2005. A master regulator for biofilm
617 formation by *Bacillus subtilis*. *Molecular Microbiology* 55:739–749.
- 618 11. Marlow VL, Porter M, Hobley L, Kiley TB, Swedlow JR, Davidson FA, Stanley-Wall NR. 2014.
619 Phosphorylated DegU Manipulates Cell Fate Differentiation in the *Bacillus subtilis* Biofilm. *J
620 Bacteriol* 196:16–27.
- 621 12. Higgins D, Dworkin J. 2012. Recent progress in *Bacillus subtilis* sporulation. *FEMS
622 Microbiology Reviews* 36:131–148.
- 623 13. Piggot PJ, Hilbert DW. 2004. Sporulation of *Bacillus subtilis*. *Current Opinion in Microbiology*
624 7:579–586.
- 625 14. González-Pastor JE. 2011. Cannibalism: a social behavior in sporulating *Bacillus subtilis*.
626 *FEMS Microbiology Reviews* 35:415–424.
- 627 15. Papenfort K, Bassler BL. 2016. Quorum sensing signal–response systems in Gram-negative
628 bacteria. *Nature Reviews Microbiology* 14:nrmicro.2016.89.
- 629 16. Jenal U, Reinders A, Lori C. 2017. **Cyclic di-GMP**: second messenger extraordinaire. *Nature
630 Reviews Microbiology* 15:nrmicro.2016.190.
- 631 17. Gomelsky M. 2011. cAMP, c-di-GMP, c-di-AMP and now cGMP: Bacteria use them all! *Mol
632 Microbiol* 79:562–565.

- 633 18. Hengge R, Gründling A, Jenal U, Ryan R, Yildiz F. 2016. Bacterial Signal Transduction by
634 Cyclic Di-GMP and Other Nucleotide Second Messengers. *Journal of Bacteriology* 198:15–
635 26.
- 636 19. Romling U, Galperin MY, Gomelsky M. 2013. Cyclic di-GMP: the First 25 Years of a Universal
637 Bacterial Second Messenger. *Microbiology and Molecular Biology Reviews* 77:1–52.
- 638 20. Purcell EB, Tamayo R. 2016. Cyclic diguanylate signaling in Gram-positive bacteria. *FEMS
639 Microbiol Rev* 40:753–773.
- 640 21. Römling U, Gomelsky M, Galperin MY. 2005. C-di-GMP: the dawning of a novel bacterial
641 signalling system. *Molecular Microbiology* 57:629–639.
- 642 22. Ausmees N, Mayer R, Weinhouse H, Volman G, Amikam D, Benziman M, Lindberg M. 2001.
643 Genetic data indicate that proteins containing the GGDEF domain possess diguanylate
644 cyclase activity. *FEMS Microbiology Letters* 204:163–167.
- 645 23. Chan C, Paul R, Samoray D, Amiot NC, Giese B, Jenal U, Schirmer T. 2004. Structural basis of
646 activity and allosteric control of diguanylate cyclase. *Proc Natl Acad Sci U S A* 101:17084–
647 17089.
- 648 24. Ryjenkov DA, Tarutina M, Moskvin OV, Gomelsky M. 2005. Cyclic Diguanylate Is a
649 Ubiquitous Signaling Molecule in Bacteria: Insights into Biochemistry of the GGDEF Protein
650 Domain. *J Bacteriol* 187:1792–1798.

- 651 25. Ross P, Weinhouse H, Aloni Y, Michaeli D, Weinberger-Ohana P, Mayer R, Braun S, de
652 Vroom E, van der Marel GA, van Boom JH, Benziman M. 1987. Regulation of cellulose
653 synthesis in *Acetobacter xylinum* by cyclic diguanylic acid. *Nature* 325:279–281.
- 654 26. Paul R, Weiser S, Amiot NC, Chan C, Schirmer T, Giese B, Jenal U. 2004. Cell cycle-dependent
655 dynamic localization of a bacterial response regulator with a novel di-guanylate cyclase
656 output domain. *Genes Dev* 18:715–727.
- 657 27. Hickman JW, Tifrea DF, Harwood CS. 2005. A chemosensory system that regulates biofilm
658 formation through modulation of cyclic diguanylate levels. *PNAS* 102:14422–14427.
- 659 28. Christen B, Christen M, Paul R, Schmid F, Folcher M, Jenoe P, Meuwly M, Jenal U. 2006.
660 Allosteric Control of Cyclic di-GMP Signaling. *J Biol Chem* 281:32015–32024.
- 661 29. Simm R, Morr M, Kader A, Nimtz M, Römling U. 2004. GGDEF and EAL domains inversely
662 regulate cyclic di-GMP levels and transition from sessility to motility: Cyclic di-GMP
663 turnover by GGDEF and EAL domains. *Molecular Microbiology* 53:1123–1134.
- 664 30. Tal R, Wong HC, Calhoon R, Gelfand D, Fear AL, Volman G, Mayer R, Ross P, Amikam D,
665 Weinhouse H, Cohen A, Sapir S, Ohana P, Benziman M. 1998. Three cdg Operons Control
666 Cellular Turnover of Cyclic Di-GMP in *Acetobacter xylinum*: Genetic Organization and
667 Occurrence of Conserved Domains in Isoenzymes. *J Bacteriol* 180:4416–4425.
- 668 31. Tischler AD, Camilli A. 2004. Cyclic diguanylate (c-di-GMP) regulates *Vibrio cholerae* biofilm
669 formation. *Mol Microbiol* 53:857–869.

- 670 32. Schmidt AJ, Ryjenkov DA, Gomelsky M. 2005. The Ubiquitous Protein Domain EAL Is a Cyclic
671 Diguanylate-Specific Phosphodiesterase: Enzymatically Active and Inactive EAL Domains. *J*
672 *Bacteriol* 187:4774–4781.
- 673 33. Christen M, Christen B, Folcher M, Schauerte A, Jenal U. 2005. Identification and
674 Characterization of a *Cyclic di-GMP*-specific Phosphodiesterase and Its Allosteric Control
675 by GTP. *J Biol Chem* 280:30829–30837.
- 676 34. Tamayo R, Tischler AD, Camilli A. 2005. The EAL Domain Protein VieA Is a Cyclic Diguanylate
677 Phosphodiesterase. *J Biol Chem* 280:33324–33330.
- 678 35. Galperin MY, Nikolskaya AN, Koonin EV. 2001. Novel domains of the prokaryotic two-
679 component signal transduction systems. *FEMS Microbiology Letters* 203:11–21.
- 680 36. Galperin MY, Natale DA, Aravind L, Koonin EV. 1999. A specialized version of the HD
681 hydrolase domain implicated in signal transduction. *Journal of molecular microbiology and*
682 *biotechnology* 1:303–305.
- 683 37. Hammer BK, Bassler BL. 2009. Distinct Sensory Pathways in *Vibrio cholerae* El Tor and
684 Classical Biotypes Modulate Cyclic Dimeric GMP Levels To Control Biofilm Formation.
685 *Journal of Bacteriology* 191:169–177.
- 686 38. Miner KD, Kurtz DM. 2016. Active Site Metal Occupancy and *Cyclic Di-GMP*
687 Phosphodiesterase Activity of *Thermotoga maritima* HD-GYP. *Biochemistry* 55:970–979.

- 688 39. Cohen D, Mechold U, Nevenzal H, Yarmiyahu Y, Randall TE, Bay DC, Rich JD, Parsek MR,
689 Kaever V, Harrison JJ, Banin E. 2015. Oligoribonuclease is a central feature of cyclic
690 diguanylate signaling in *Pseudomonas aeruginosa*. PNAS 112:11359–11364.
- 691 40. Orr MW, Donaldson GP, Severin GB, Wang J, Sintim HO, Waters CM, Lee VT. 2015.
692 Oligoribonuclease is the primary degradative enzyme for pGpG in *Pseudomonas*
693 *aeruginosa* that is required for cyclic-di-GMP turnover. Proc Natl Acad Sci USA 112:E5048–
694 5057.
- 695 41. Orr MW, Weiss CA, Severin GB, Turdiev H, Kim S-K, Turdiev A, Liu K, Tu BP, Waters CM,
696 Winkler WC, Lee VT. 2018. A Subset of Exoribonucleases Serve as Degradative Enzymes for
697 pGpG in c-di-GMP Signaling. Journal of Bacteriology 200.
- 698 42. Tatusov RL, Galperin MY, Natale DA, Koonin EV. 2000. The COG database: a tool for
699 genome-scale analysis of protein functions and evolution. Nucleic Acids Res 28:33–36.
- 700 43. Chou S-H, Galperin MY. 2015. Diversity of Cyclic Di-GMP-Binding Proteins and Mechanisms.
701 J Bacteriol 198:32–46.
- 702 44. Nelson JW, Breaker RR. 2017. The lost language of the RNA World. Sci Signal 10:eaam8812.
- 703 45. Sudarsan N, Lee ER, Weinberg Z, Moy RH, Kim JN, Link KH, Breaker RR. 2008. Riboswitches
704 in Eubacteria Sense the Second Messenger Cyclic Di-GMP. Science 321:411–413.
- 705 46. Henkin TM. 2008. Riboswitch RNAs: using RNA to sense cellular metabolism. Genes Dev
706 22:3383–3390.

- 707 47. Ramesh A. 2015. Second messenger – Sensing riboswitches in bacteria. Seminars in Cell &
708 Developmental Biology 47–48:3–8.
- 709 48. Lee ER, Sudarsan N, Breaker RR. 2010. Riboswitches That Sense Cyclic Di-GMP. The Second
710 Messenger Cyclic Di-GMP 215–229.
- 711 49. Chen Y, Chai Y, Guo J -h., Losick R. 2012. Evidence for Cyclic Di-GMP-Mediated Signaling in
712 *Bacillus subtilis*. Journal of Bacteriology 194:5080–5090.
- 713 50. Gao X, Mukherjee S, Matthews PM, Hammad LA, Kearns DB, Dann CE. 2013. Functional
714 Characterization of Core Components of the *Bacillus subtilis* Cyclic-Di-GMP Signaling
715 Pathway. Journal of Bacteriology 195:4782–4792.
- 716 51. Subramanian S, Gao X, Dann CE, Kearns DB. 2017. MotI (DgrA) acts as a molecular clutch on
717 the flagellar stator protein MotA in *Bacillus subtilis*. PNAS 114:13537–13542.
- 718 52. Bedrunka P, Graumann PL. 2017. New Functions and Subcellular Localization Patterns of c-
719 di-GMP Components (GGDEF Domain Proteins) in *B. subtilis*. Front Microbiol 8.
- 720 53. Bedrunka P, Graumann PL. 2017. Subcellular clustering of a putative c-di-GMP-dependent
721 exopolysaccharide machinery affecting macro colony architecture in *Bacillus subtilis*.
722 Environmental Microbiology Reports 9:211–222.
- 723 54. Minasov G, Padavattan S, Shuvalova L, Brunzelle JS, Miller DJ, Baslé A, Massa C, Collart FR,
724 Schirmer T, Anderson WF. 2009. Crystal Structures of YkuL and Its Complex with Second

- 725 Messenger Cyclic Di-GMP Suggest Catalytic Mechanism of Phosphodiester Bond Cleavage
726 by EAL Domains. *J Biol Chem* 284:13174–13184.
- 727 55. Chandrangsu P, Helmann JD. 2016. Intracellular Zn(II) Intoxication Leads to Dysregulation of
728 the PerR Regulon Resulting in Heme Toxicity in *Bacillus subtilis*. *PLOS Genetics*
729 12:e1006515.
- 730 56. Aguilar C, Vlamakis H, Losick R, Kolter R. 2007. Thinking about *Bacillus subtilis* as a
731 multicellular organism. *Current Opinion in Microbiology* 10:638–643.
- 732 57. Grangemard I, Wallach J, Maget-Dana R, Peypoux F. 2001. Lichenysin. *Appl Biochem
733 Biotechnol* 90:199–210.
- 734 58. Sen R. 2010. Surfactin: biosynthesis, genetics and potential applications. *Adv Exp Med Biol*
735 672:316–323.
- 736 59. Veith B, Herzberg C, Steckel S, Feesche J, Maurer KH, Ehrenreich P, Bäumer S, Henne A,
737 Liesegang H, Merkl R, Ehrenreich A, Gottschalk G. 2004. The Complete Genome Sequence
738 of *Bacillus licheniformis* DSM13, an Organism with Great Industrial Potential. *MMB* 7:204–
739 211.
- 740 60. Serganov A, Nudler E. 2013. A Decade of Riboswitches. *Cell* 152:17–24.
- 741 61. Winkler WC, Breaker RR. 2005. Regulation of Bacterial Gene Expression by Riboswitches.
742 *Annual Review of Microbiology* 59:487–517.

- 743 62. Paige JS, Wu KY, Jaffrey SR. 2011. RNA Mimics of Green Fluorescent Protein. *Science*
744 333:642–646.
- 745 63. You M, Jaffrey SR. 2015. Structure and Mechanism of RNA Mimics of Green Fluorescent
746 Protein. *Annu Rev Biophys* 44:187–206.
- 747 64. Kellenberger CA, Hammond MC. 2015. In Vitro Analysis of Riboswitch–Spinach Aptamer
748 Fusions as Metabolite-Sensing Fluorescent Biosensors, p. 147–172. *In Methods in*
749 *Enzymology*. Elsevier.
- 750 65. Ponchon L, Dardel F. 2007. Recombinant RNA technology: the tRNA scaffold. *Nat Meth*
751 4:571–576.
- 752 66. You M, Litke JL, Jaffrey SR. 2015. Imaging metabolite dynamics in living cells using a
753 Spinach-based riboswitch. *Proc Natl Acad Sci USA* 112:E2756–2765.
- 754 67. Wickiser JK, Winkler WC, Breaker RR, Crothers DM. 2005. The speed of RNA transcription
755 and metabolite binding kinetics operate an FMN riboswitch. *Mol Cell* 18:49–60.
- 756 68. Smith KD, Lipchock SV, Strobel SA. 2012. Structural and biochemical characterization of
757 linear dinucleotide analogues bound to the c-di-GMP-I aptamer. *Biochemistry* 51:425–432.
- 758 69. Eichenberger P, Jensen ST, Conlon EM, van Ooij C, Silvaggi J, González-Pastor J-E, Fujita M,
759 Ben-Yehuda S, Stragier P, Liu JS, Losick R. 2003. The σE Regulon and the Identification of
760 Additional Sporulation Genes in *Bacillus subtilis*. *Journal of Molecular Biology* 327:945–
761 972.

- 762 70. Cutting S, Driks A, Schmidt R, Kunkel B, Losick R. 1991. Forespore-specific transcription of a
763 gene in the signal transduction pathway that governs Pro-sigma K processing in *Bacillus*
764 *subtilis*. *Genes Dev* 5:456–466.
- 765 71. Camp AH, Losick R. 2009. A feeding tube model for activation of a cell-specific transcription
766 factor during sporulation in *Bacillus subtilis*. *Genes Dev* 23:1014–1024.
- 767 72. Roels S, Driks A, Losick R. 1992. Characterization of *spoIVA*, a sporulation gene involved in
768 coat morphogenesis in *Bacillus subtilis*. *Journal of Bacteriology* 174:575–585.
- 769 73. Zheng L, Halberg R, Roels S, Ichikawa H, Kroos L, Losick R. 1992. Sporulation regulatory
770 protein *gerE* from *Bacillus subtilis* binds to and can activate or repress transcription from
771 promoters for mother-cell-specific genes. *Journal of Molecular Biology* 226:1037–1050.
- 772 74. Cutting S, Panzer S, Losick R. 1989. Regulatory studies on the promoter for a gene governing
773 synthesis and assembly of the spore coat in *Bacillus subtilis*. *Journal of Molecular Biology*
774 207:393–404.
- 775 75. Branda SS, González-Pastor JE, Ben-Yehuda S, Losick R, Kolter R. 2001. Fruiting body
776 formation by *Bacillus subtilis*. *Proceedings of the National Academy of Sciences* 98:11621–
777 11626.
- 778 76. Chai Y, Kolter R, Losick R. 2010. Reversal of an epigenetic switch governing cell chaining in
779 *Bacillus subtilis* by protein instability. *Molecular Microbiology* 78:218–229.

- 780 77. Chai Y, Kolter R, Losick R. 2009. Paralogous antirepressors acting on the master regulator
781 for biofilm formation in *Bacillus subtilis*. *Molecular Microbiology* 74:876–887.
- 782 78. Fang X, Gomelsky M. 2010. A post-translational, c-di-GMP-dependent mechanism
783 regulating flagellar motility. *Molecular Microbiology* 76:1295–1305.
- 784 79. Paul K, Nieto V, Carlquist WC, Blair DF, Harshey RM. 2010. The c-di-GMP Binding Protein
785 YcgR Controls Flagellar Motor Direction and Speed to Affect Chemotaxis by a “Backstop
786 Brake” Mechanism. *Mol Cell* 38:128–139.
- 787 80. Boehm A, Kaiser M, Li H, Spangler C, Kasper CA, Ackermann M, Kaever V, Sourjik V, Roth V,
788 Jenal U. 2010. Second Messenger-Mediated Adjustment of Bacterial Swimming Velocity.
789 *Cell* 141:107–116.
- 790 81. Molle V, Fujita M, Jensen ST, Eichenberger P, González-Pastor JE, Liu JS, Losick R. 2003. The
791 SpoOA regulon of *Bacillus subtilis*. *Molecular Microbiology* 50:1683–1701.
- 792 82. Fagerlund A, Smith V, Røhr ÅK, Lindbäck T, Parmer MP, Andersson KK, Reubaet L, Økstad
793 OA. 2016. Cyclic diguanylate regulation of *Bacillus cereus* group biofilm formation.
794 *Molecular Microbiology* 101:471–494.
- 795 83. Tran NT, Hengst CDD, Gomez-Escribano JP, Buttner MJ. 2011. Identification and
796 Characterization of **CdgB**, a Diguanylate Cyclase Involved in Developmental Processes in
797 *Streptomyces coelicolor*. *Journal of Bacteriology* 193:3100–3108.

- 798 84. Den Hengst CD, Tran NT, Bibb MJ, Chandra G, Leskiw BK, Buttner MJ. 2010. Genes essential
799 for morphological development and antibiotic production in *Streptomyces coelicolor* are
800 targets of BluD during vegetative growth. *Molecular Microbiology* 78:361–379.
- 801 85. Hull TD, Ryu M-H, Sullivan MJ, Johnson RC, Klena NT, Geiger RM, Gomelsky M, Bennett JA.
802 2012. Cyclic Di-GMP Phosphodiesterases RmdA and RmdB Are Involved in Regulating
803 Colony Morphology and Development in *Streptomyces coelicolor*. *Journal of Bacteriology*
804 194:4642–4651.
- 805 86. Tschowri N, Schumacher MA, Schlimpert S, Chinnam NB, Findlay KC, Brennan RG, Buttner
806 MJ. 2014. Tetrameric c-di-GMP mediates effective transcription factor dimerization to
807 control *Streptomyces* development. *Cell* 158:1136–1147.
- 808 87. D’Souza C, Nakano MM, Zuber P. 1994. Identification of comS, a gene of the srfA operon
809 that regulates the establishment of genetic competence in *Bacillus subtilis*. *Proc Natl Acad
810 Sci U S A* 91:9397–9401.
- 811 88. Nakano MM, Zuber P. 1989. Cloning and characterization of srfB, a regulatory gene involved
812 in surfactin production and competence in *Bacillus subtilis*. *J Bacteriol* 171:5347–5353.
- 813 89. Hamoen LW, Venema G, Kuipers OP. 2003. Controlling competence in *Bacillus subtilis*:
814 shared use of regulators. *Microbiology* 149:9–17.
- 815 90. Dubnau D. 1991. Genetic competence in *Bacillus subtilis*. *Microbiology and Molecular
816 Biology Reviews* 55:395–424.

- 817 91. Lopez D, Vlamakis H, Losick R, Kolter R. 2009. Paracrine signaling in a bacterium. *Genes &*
818 *Development* 23:1631–1638.
- 819 92. Yakimov MM, Golyshin PN. 1997. ComA-Dependent Transcriptional Activation of Lichenysin
820 A Synthetase Promoter in *Bacillus subtilis* cells. *Biotechnology Progress* 13:757–761.
- 821 93. Jakobs M, Hoffmann K, Liesegang H, Volland S, Meinhardt F. 2015. The two putative comS
822 homologs of the biotechnologically important *Bacillus licheniformis* do not contribute to
823 competence development. *Appl Microbiol Biotechnol* 99:2255–2266.
- 824 94. Christen M, Kulasekara HD, Christen B, Kulasekara BR, Hoffman LR, Miller SI. 2010.
825 Asymmetrical Distribution of the Second Messenger c-di-GMP upon Bacterial Cell Division.
826 *Science* 328:1295–1297.
- 827 95. Kulasekara BR, Kamischke C, Kulasekara HD, Christen M, Wiggins PA, Miller SI. 2013. c-di-
828 GMP heterogeneity is generated by the chemotaxis machinery to regulate flagellar
829 motility. *eLife* 2.
- 830 96. Abel S, Bucher T, Nicollier M, Hug I, Kaever V, Abel zur Wiesch P, Jenal U. 2013. Bi-modal
831 Distribution of the Second Messenger c-di-GMP Controls Cell Fate and Asymmetry during
832 the Caulobacter Cell Cycle. *PLoS Genet* 9.
- 833 97. Kellenberger CA, Sales-Lee J, Pan Y, Gassaway MM, Herr AE, Hammond MC. 2015. A
834 minimalist biosensor: Quantitation of cyclic di-GMP using the conformational change of a
835 riboswitch aptamer. *RNA Biology* 12:1189–1197.

- 836 98. Zhang J, Fei J, Leslie BJ, Han KY, Kuhlman TE, Ha T. 2015. Tandem Spinach Array for mRNA
837 Imaging in Living Bacterial Cells. *Sci Rep* 5.
- 838 99. Süel GM, Kulkarni RP, Dworkin J, Garcia-Ojalvo J, Elowitz MB. 2007. Tunability and Noise
839 Dependence in Differentiation Dynamics. *Science* 315:1716–1719.
- 840 100. Campo N, Rudner DZ. 2007. SpoIVB and CtpB Are Both Forespore Signals in the Activation
841 of the Sporulation Transcription Factor K in *Bacillus subtilis*. *Journal of Bacteriology*
842 189:6021–6027.
- 843 101. Dann CE, Wakeman CA, Sieling CL, Baker SC, Irnov I, Winkler WC. 2007. Structure and
844 Mechanism of a Metal-Sensing Regulatory RNA. *Cell* 130:878–892.
- 845 102. Konkol MA, Blair KM, Kearns DB. 2013. Plasmid-Encoded ComI Inhibits Competence in the
846 Ancestral 3610 Strain of *Bacillus subtilis*. *Journal of Bacteriology* 195:4085–4093.
- 847 103. Gibson DG, Young L, Chuang R-Y, Venter JC, Hutchison III CA, Smith HO. 2009. Enzymatic
848 assembly of DNA molecules up to several hundred kilobases. *Nature Methods* 6:343–345.
- 849 104. Veening J-W, Smits WK, Hamoen LW, Kuipers OP. 2006. Single cell analysis of gene
850 expression patterns of competence development and initiation of sporulation in *Bacillus*
851 *subtilis* grown on chemically defined media. *Journal of Applied Microbiology* 101:531–541.
- 852 105. Smits WK, Eschevins CC, Susanna KA, Bron S, Kuipers OP, Hamoen LW. 2005. Stripping
853 *Bacillus*: ComK auto-stimulation is responsible for the bistable response in competence
854 development. *Molecular Microbiology* 56:604–614.

- 855 106. Koo B-M, Kritikos G, Farelli JD, Todor H, Tong K, Kimsey H, Wapinski I, Galardini M, Cabal A,
856 Peters JM, Hachmann A-B, Rudner DZ, Allen KN, Typas A, Gross CA. 2017. Construction and
857 Analysis of Two Genome-scale Deletion Libraries for *Bacillus subtilis*. *Cell Syst* 4:291-
858 305.e7.
- 859 107. Jarmer H, Berka R, Knudsen S, Saxild HH. 2002. Transcriptome analysis documents induced
860 competence of *Bacillus subtilis* during nitrogen limiting conditions. *FEMS Microbiol Lett*
861 206:197–200.
- 862 108. Paintdakhi A, Parry B, Campos M, Irnov I, Elf J, Surovtsev I, Jacobs-Wagner C. 2016. Oufti:
863 an integrated software package for high-accuracy, high-throughput quantitative
864 microscopy analysis. *Molecular microbiology* 99:767–777.
- 865 109. Schindelin J, Arganda-Carreras I, Frise E, Kaynig V, Longair M, Pietzsch T, Preibisch S,
866 Rueden C, Saalfeld S, Schmid B, Tinevez J-Y, White DJ, Hartenstein V, Eliceiri K, Tomancak
867 P, Cardona A. 2012. Fiji - an Open Source platform for biological image analysis. *Nat
868 Methods* 9.

869
870 **Figure Legends**

871 **Figure 1. The *IchAA* riboswitch promotes transcription termination in response to
872 c-di-GMP.** (A) Schematic of the mechanism of regulation by the *B. licheniformis IchAA*
873 riboswitch in response to high and low levels of c-di-GMP. (B) A transcription
874 termination assay of the *IchAA* UTR RNA with increasing concentrations of c-di-GMP (0
875 to 1000 µM) shows premature termination of run-off (RO) within the leader sequence,

876 as compared to a terminated (T) transcript. (C) Schematic of the Spinach2 RNA
877 allosterically regulated by the *lchAA* riboswitch aptamer in response to c-di-GMP. (D) *In*
878 *vitro* fluorescence assay of the riboswitch-Spinach2 RNA (100 nM) in the presence of
879 saturating DFHBI (10 μ M) and increasing concentrations of c-di-GMP or pGpG. Binding
880 affinity measurements are representative of two independent replicates.

881

882 **Figure 2. Expression of a *lchAA* riboswitch-*yfp* reporter *in vivo* results in bimodal
883 distribution of fluorescence.** (A) Representative microscopy images of wild-type *B.*
884 *subtilis* PY79 expressing a constitutive $P_{\text{const}}\text{-}yfp$ reporter, a riboswitch reporter construct
885 $P_{\text{const}}\text{-riboswitch-}yfp$, or a riboswitch reporter construct comprising a deletion
886 corresponding to the riboswitch aptamer ($P_{\text{const}}\text{-riboswitch}^{\Delta\text{apt}}\text{-}yfp$). (B) Histograms of the
887 quantification of fluorescence intensity per cell of wild-type *B. subtilis* PY79 expressing
888 $P_{\text{const}}\text{-}yfp$ compared to $P_{\text{const}}\text{-riboswitch-}yfp$ or (C) $P_{\text{const}}\text{-}yfp$ compared to $P_{\text{const}}\text{-}$
889 riboswitch $^{\Delta\text{apt}}\text{-}yfp$ (n~300).

890

891 **Figure 3. Deletion of *pdeH* results in increased c-di-GMP.** (A) Representative
892 microscopy images of *B. subtilis* PY79 wild-type (WT) or $\Delta pdeH$ expressing the
893 constitutive $P_{\text{const}}\text{-}yfp$ reporter, or (B) the riboswitch reporter construct $P_{\text{const}}\text{-}$ riboswitch-
894 *yfp*. (C-D) Histograms of the quantification of fluorescence intensity per cell comparing
895 *B. subtilis* PY79 WT or $\Delta pdeH$ expressing $P_{\text{const}}\text{-}yfp$ or $P_{\text{const}}\text{-riboswitch-}yfp$ (n~300).

896

897 **Figure 4. Expression of the riboswitch reporter varies nonrandomly among *B.*
898 *subtilis* cell types.** (A) Representative microscopy images of wild-type *B. subtilis* PY79

899 expressing the riboswitch reporter construct P_{const^-} riboswitch-*mCherry* and the motility
900 reporter $P_{hag^-}gfp$. Statistical analyses show these reporters are significantly correlated
901 ($****P<0.0001$). (B) Expression of P_{const^-} riboswitch-*mCherry* and the biofilm reporter
902 $P_{tapA^-}yfp$ are anti-correlated ($**P=0.0039$). (C) Expression of P_{const^-} riboswitch-*mCherry*
903 and the competence reporter $P_{comG^-}yfp$ are correlated ($****P<0.0001$). (D-F)
904 Quantification of the fluorescence intensity per cell of P_{const^-} riboswitch-*mCherry*
905 compared to each cell type reporter in each construct (n~300). Dotted lines represent
906 the cut-off that divides fluorescent cells from non-fluorescent cells. Statistical
907 significance determined by chi-square analysis.

908

909 **Figure 5. High c-di-GMP levels correlate with sporulation.** Representative
910 microscopy images of a time course through sporulation of the wild-type *B. subtilis*
911 PY79 expressing the riboswitch reporter construct P_{const^-} riboswitch-*yfp* and a
912 constitutive reporter $P_{const^-}mCherry$.

913

914 **Figure 6. Deletion of *pdeH* does not change expression of each cell type reporter.**
915 (A) Representative microscopy images of *B. subtilis* PY79 wild-type (WT) or $\Delta pdeH$
916 expressing the riboswitch reporter construct P_{const^-} riboswitch-*mCherry* and the motility
917 reporter $P_{hag^-}gfp$, or (B) P_{const^-} riboswitch-*mCherry* and the biofilm reporter $P_{tapA^-}yfp$, or
918 (C) P_{const^-} riboswitch-*mCherry* and the competence reporter $P_{comG^-}yfp$. (D-F)
919 Quantification of the fluorescence intensity per cell of P_{const^-} riboswitch-*mCherry*
920 compared to each cell type reporter, expressed in *B. subtilis* PY79 WT or $\Delta pdeH$
921 (n~300).

922

923 **Figure 7. Deletion of global regulators affects *pdeH* expression and c-di-GMP**

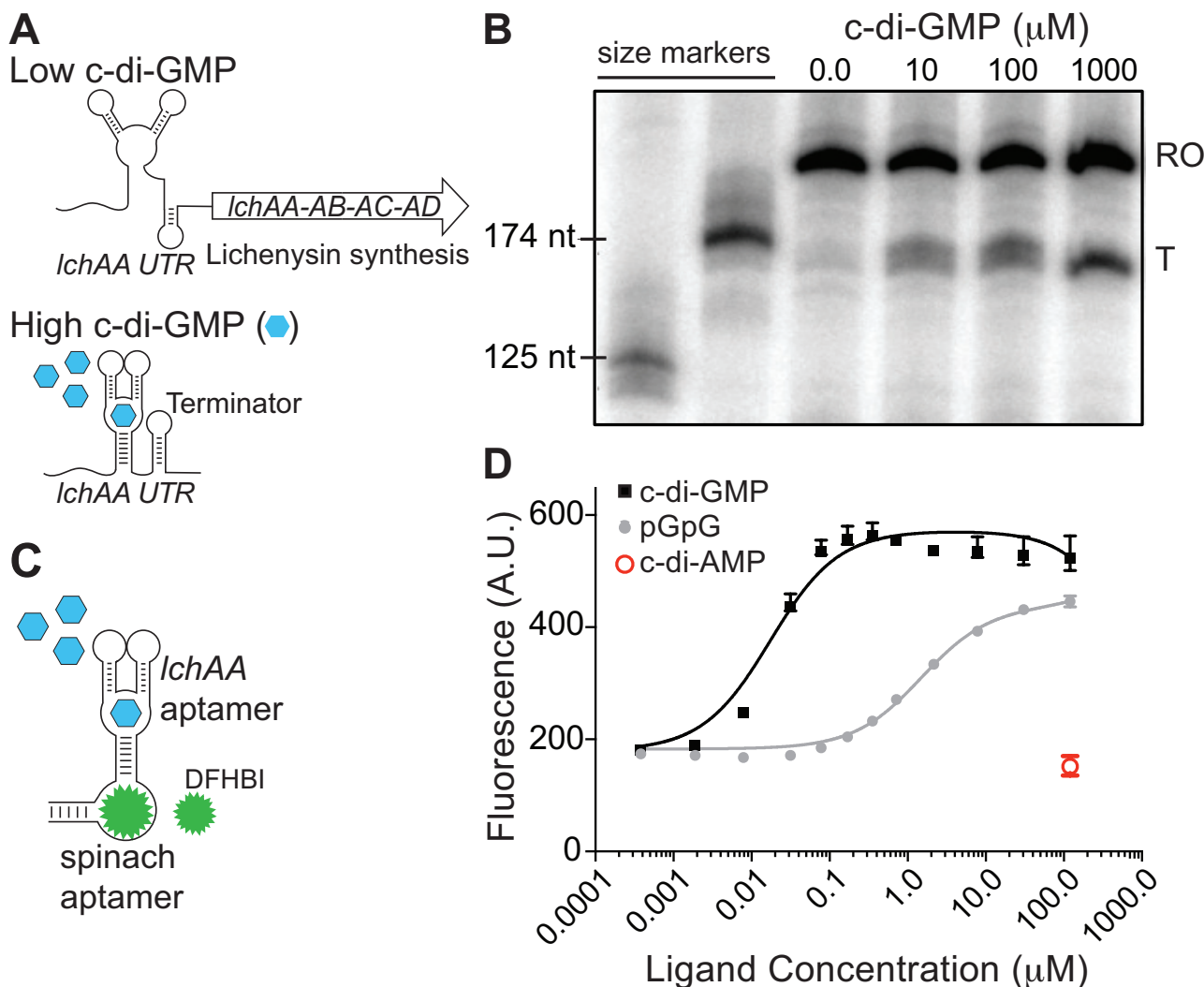
924 **levels.** Quantification of the fluorescence intensity per cell of $P_{pdeH}\text{-sf-gfp}$ in *B. subtilis*

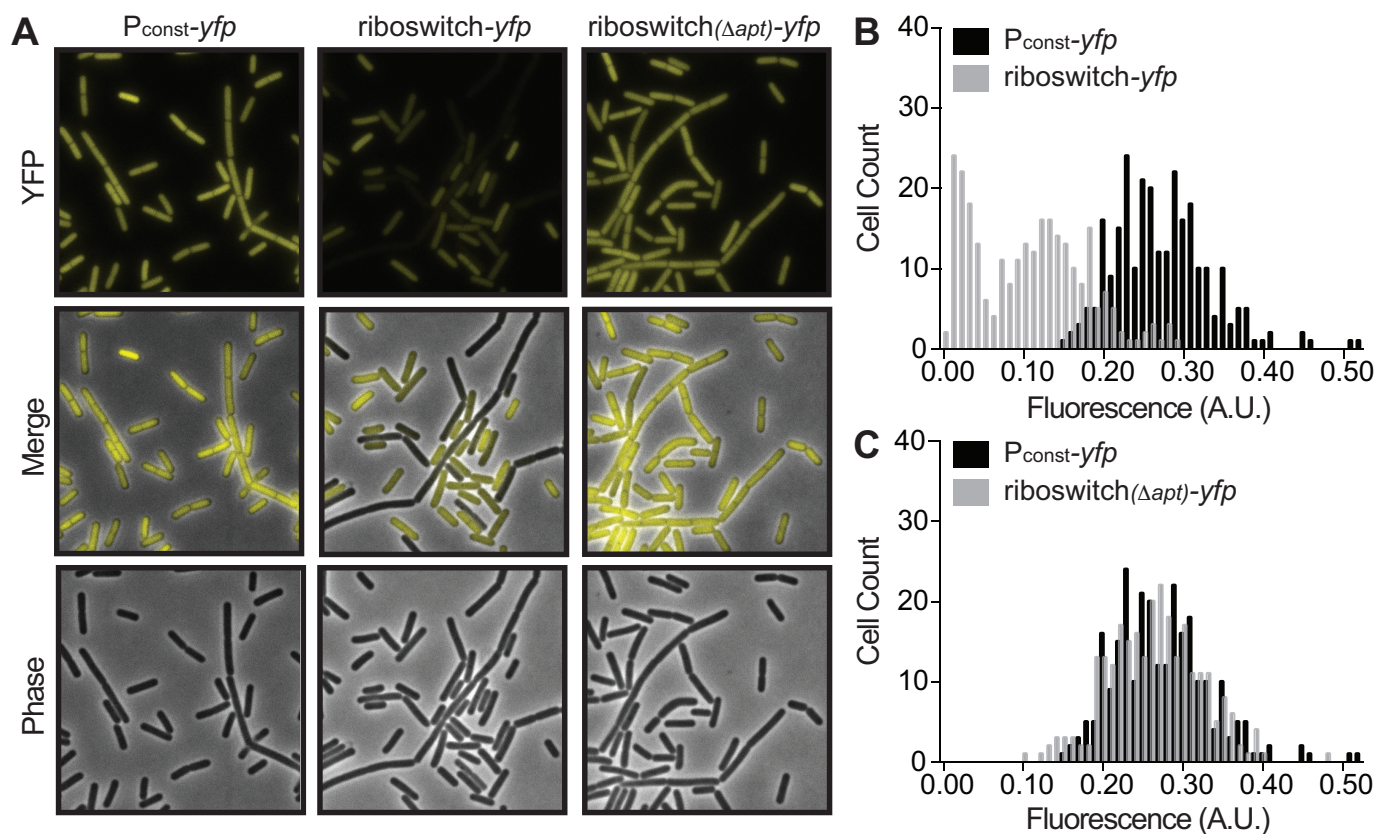
925 PY79 wild-type (WT), and (A) $\Delta spoOA$, (B) $\Delta sinR$, or (C) $\Delta sigD$ genetic backgrounds

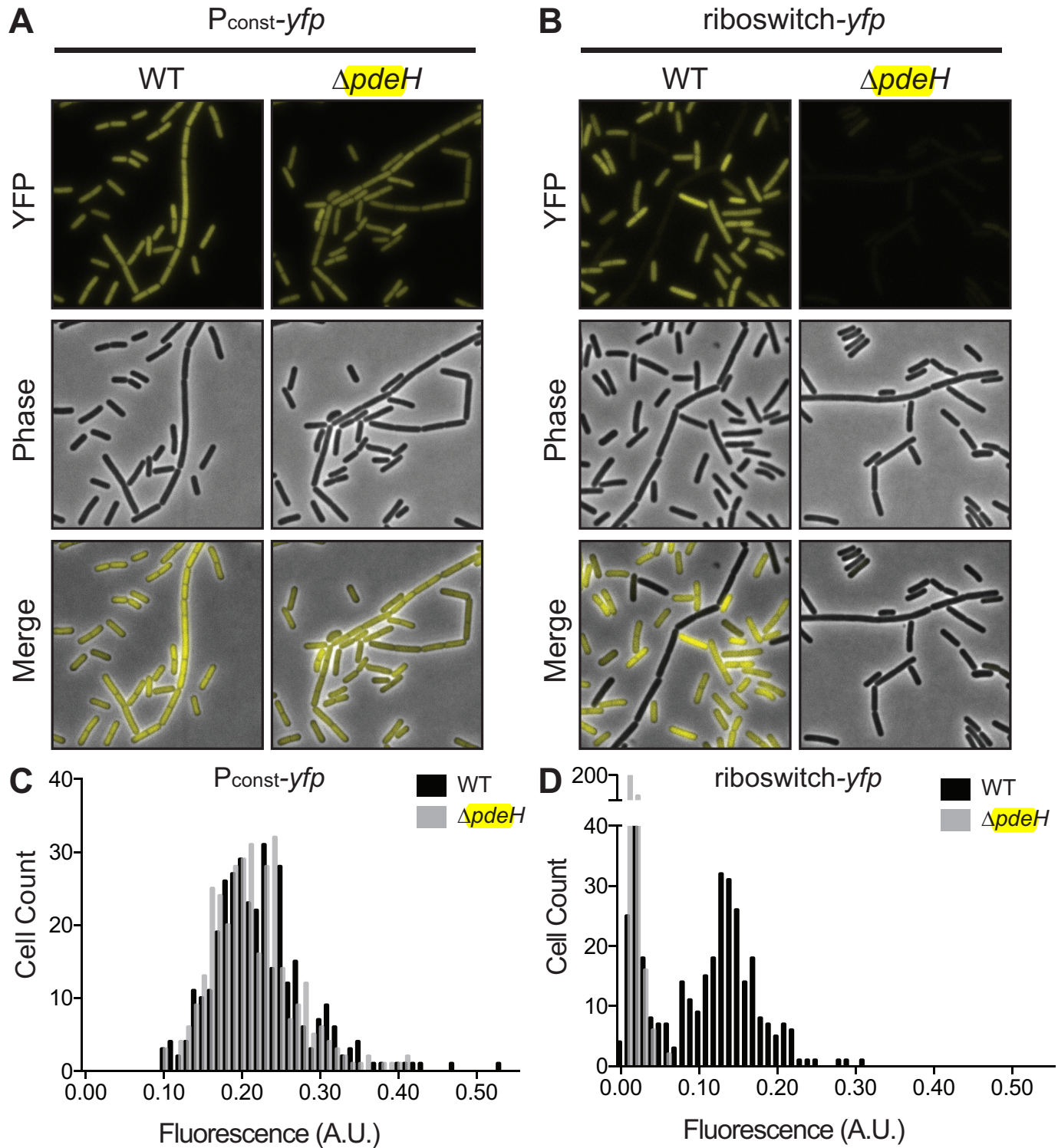
926 (n~300). Quantification and comparison of the fluorescence intensity per cell of P_{const} -

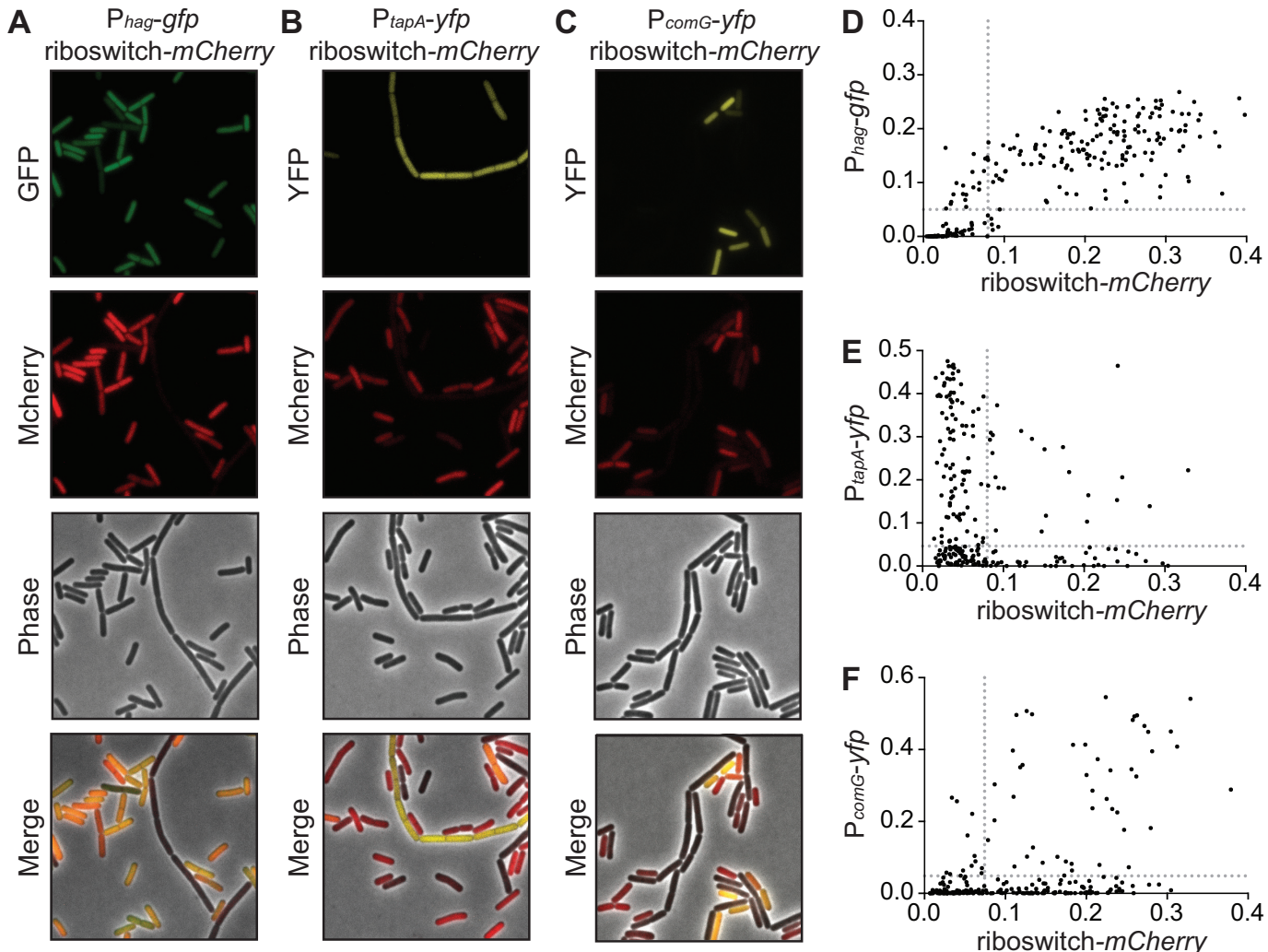
927 riboswitch-*mCherry* in *B. subtilis* PY79 wild-type (WT), and (D) $\Delta spoOA$, (E) $\Delta sinR$, or

928 (F) $\Delta sigD$ genetic backgrounds (n~500).









$P_{\text{const}}\text{-}m\text{Cherry}$
riboswitch-*yfp*

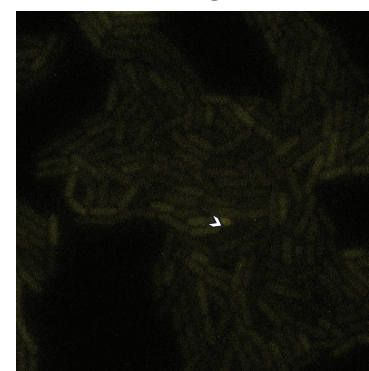
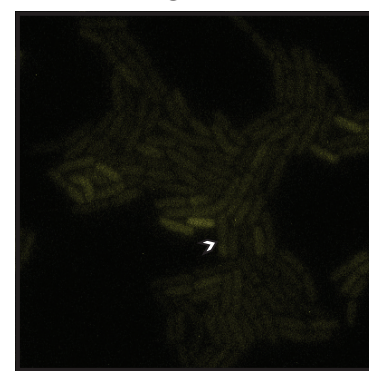
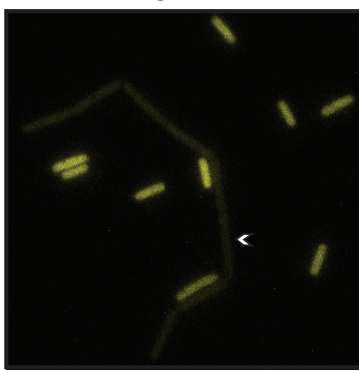
time into sporulation

0 hr

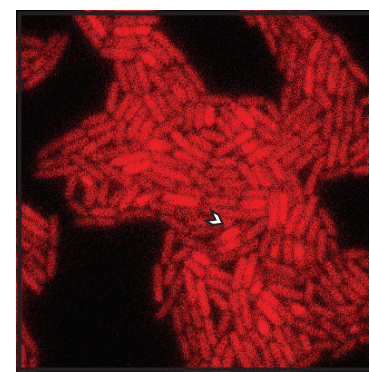
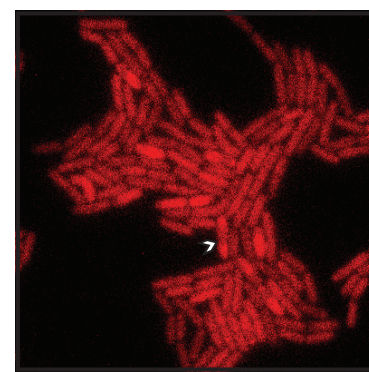
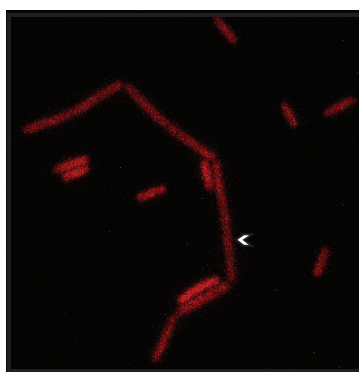
9 hr

18 hr

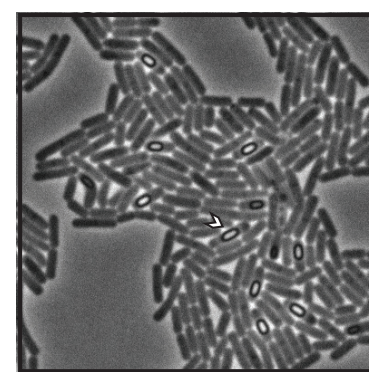
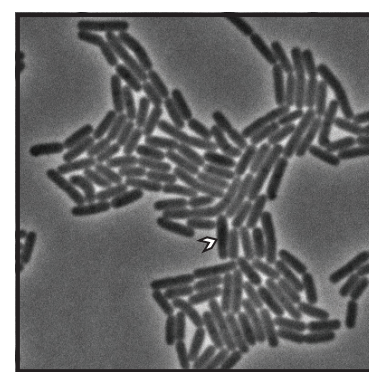
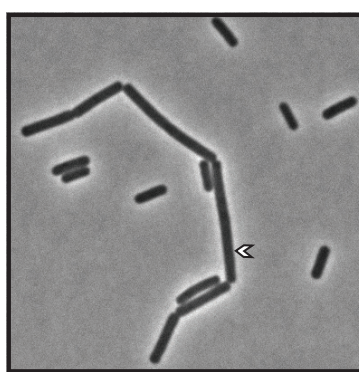
YFP



Mcherry



Phase



Merge

